

Quatorzième Congrès  
des Grands Barrages  
*Rio de Janeiro, 1982*

## **LARGE-SCALE LABORATORY TESTS FOR THE MECHANICAL CHARACTERIZATION OF GRANULAR MATERIALS FOR EMBANKMENT DAMS (\*)**

Alberto FRASSONI

*Rock Mechanics Dpt. — ISMES, Bergamo*

Ulrich HEGG

*Geotechnic Dpt. ELC — Electroconsult, Milano*

Pier Paolo ROSSI

*Rock Mechanics Dpt. — ISMES, Bergamo*

ITALY

### **1. INTRODUCTION**

The problem of defining meaningful deformational parameters for the design of earth and rockfill structures has been a demanding task for the soils engineer concerned with such structures since the concept of deformational analyses has got hold of design in the field of soil mechanics. While the problem is difficult enough when dealing with homogeneous soils, it becomes extremely untractable when dealing with rockfill or heterogeneous earth fill materials.

The possibilities of determining design input parameters in the latter case are basically two: the performance of large scale laboratory tests or the back analysis of the behaviour of existing instrumented earth and rockfill structures. There is little doubt that the analysis of full scale structures is the best source of information, but the available information for a specific design problem is generally scarce and not normally ready at hand. In these circumstances, large scale laboratory tests are considered a practical

---

(\*) *Essai de laboratoire à grande échelle pour déterminer les caractéristiques mécaniques des matériaux granulaires pour barrages en remblai.*

and, also in economical terms, acceptable solution. They, too, pose their problems, like laboratory technology, shipping of large quantities of material to the laboratory and various questions related to sample preparation and evaluation of test results; but as is hoped this paper will show, a wide range of useful results can be obtained for all kinds of materials with apparatuses which are relatively simple.

Emphasis is placed in this paper on the description of a large scale oedometer designed and constructed by ISMES (Experimental Institute of Models and Structures, Bergamo, Italy) for the testing of coarse grained materials. Its main features are, apart from the size of the apparatus, the reduction of side friction by a system of lateral confinement which is deformable (vertically), the possibility of measuring horizontal stresses, the application of back-pressures and the execution of constant head permeability tests. The apparatus is thought to be noteworthy because of the relative simplicity of the testing procedures involved which allows its installation also in a well equipped field laboratory. Because a complete definition of stress-strain parameters requires also triaxial testing, some consideration is given to this type of large scale tests.

After the description of the apparatuses, the paper gives some comments on criteria and methods for the preparation of representative samples. Finally, after examining the influence of some mechanical characteristics of test materials, a detailed summary is presented of the results of some tests that have been carried out for a few actual design jobs. All considered cases regard earth and rockfill embankments. The reported large scale laboratory tests were carried out to furnish input parameters for finite element analyses.

## 2. TEST APPARATUSES

### 2.1. LARGE OEDOMETER CELL

The determination of the compressibility characteristics of granular materials by means of confined compression tests in steel cells with rigid walls is affected by significant errors due to side friction. To avoid friction effects, a special cell has been developed by ISMES with walls made of alternating rigid and deformable rings glued to one another (Fig. 1).

While rigid lateral confinement is provided by the rigid rings, the presence of highly deformable rings in between, leads to an important reduction of the lateral resistance against the axial compressive load. On the whole, the cell can be regarded to consist of a highly anisotropic material.

When compressed between two steel end plates, the chamber wall deforms together with the test material and offers a very little resistance. The amount of the side resistance can be easily deducted, for each value of axial settlement, by means of a calibration test on the empty chamber.

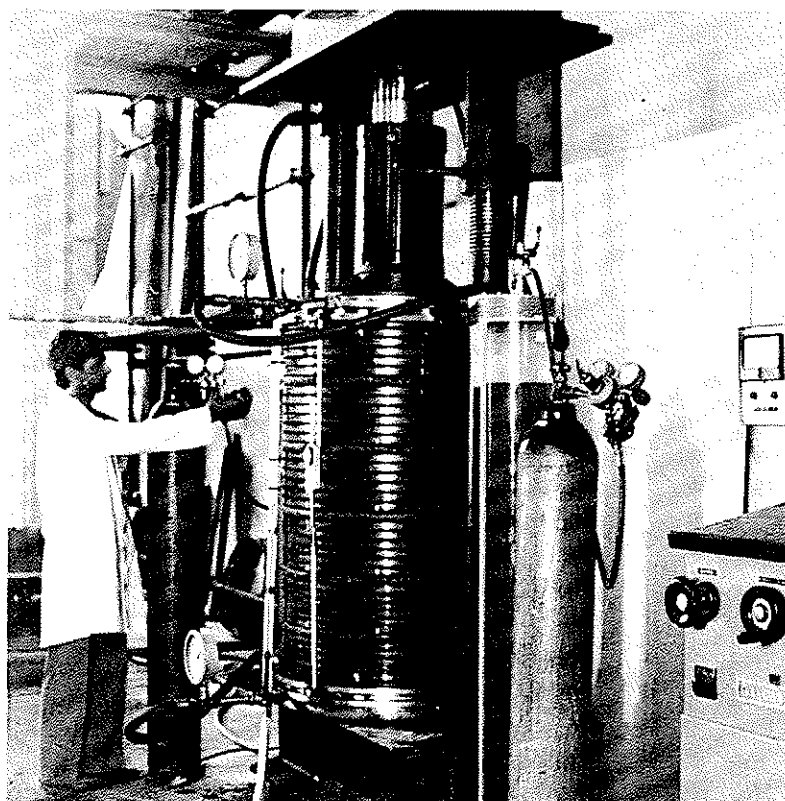


Fig. 1

View of the oedometer cell ( $\varnothing = 600$  mm,  $H = 1\,200$  mm).

*Vue de l'oédomètre ( $\varnothing = 600$  mm,  $H = 1\,200$  mm).*

Depending on the maximum grain-size of the material, the tests are carried out in cells of different diameters (up to 1 300 mm) with a height/diameter ratio equal to 2. Usually a chamber with a diameter of 500 or 600 mm is used. This requires a down-scaling of the grain-size distribution curve of the test material according to the criteria described below.

During the test it is possible to determine the value of the confining pressure applied laterally to the specimen through the measurement of the deformations of the rigid rings. Five of them are equipped with 8 strain-gauges each and act as dynamometric rings. The axial settlements of the specimens are measured by means of 4 displacement transducers (range 0-100 mm).

In the two end plates of steel a set of holes ( $\varnothing = 2$  mm) at a distance of 20 mm allows for the complete saturation of the material.

The possibilities offered by this oedometer have recently been enlarged:

The test chamber has been made watertight at either end so that pore pressures up to a maximum value of 1,0 MPa can be applied to the material.

The hydropneumatic apparatus shown in Fig. 2 is used to apply the pore-pressures. With the same loading equipment it is also possible to determine the permeability characteristics of the material under different load conditions (\*).

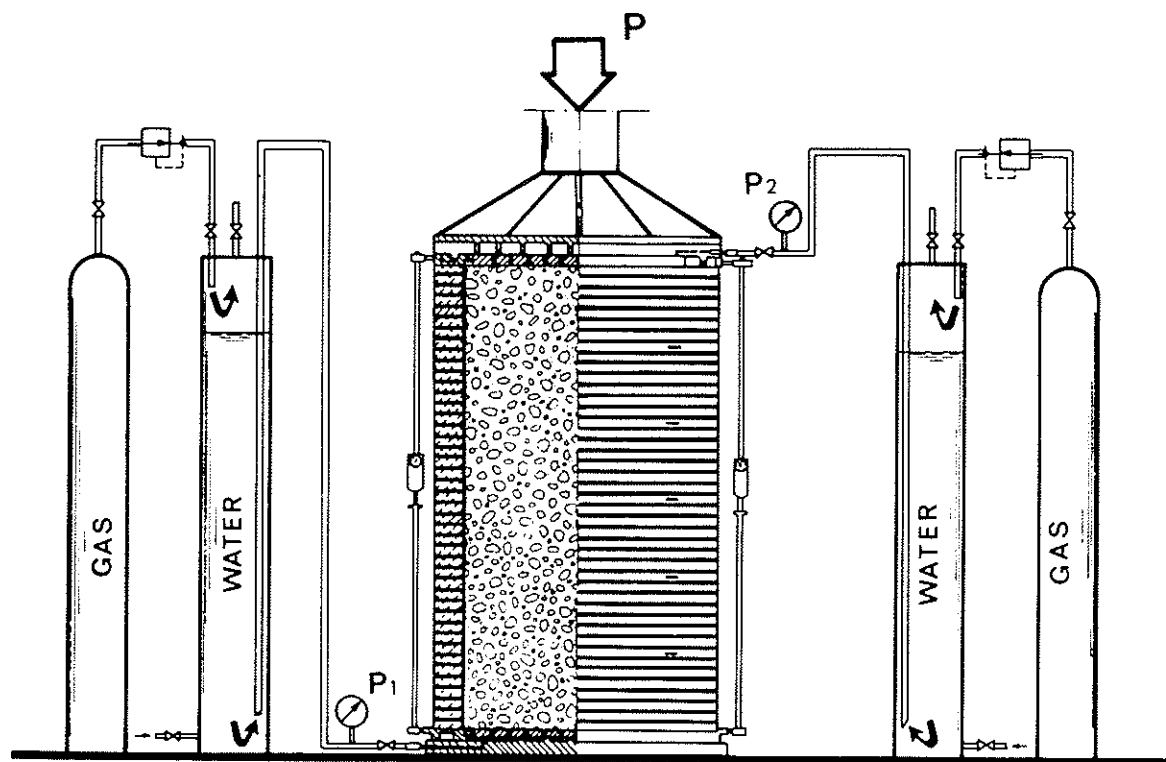


Fig. 2

Scheme of the oedometer cell with the hydropneumatic loading apparatus.

*Schéma de l'oédomètre avec l'appareillage hydropneumatique pour la charge.*

## 2.2. CONVENTIONAL TRIAXIAL TEST

For a more complete determination of the parameters which define the mechanical behaviour of the test material it is useful to have also some conventional triaxial tests carried out on specimens of large dimensions ( $\varnothing = 350$  mm,  $H = 700$  mm). The apparatus used by ISMES is illustrated in Fig. 3.

Both confining pressure and axial load are applied to the specimen by means of a loading equipment with automatic regulation. The axial defor-

(\*) The apparatuses have been realized in collaboration with ENEL (Research and Development Department).

mation is measured by inductive transducers (range 0-100 mm). Through the measurement of the volume of the liquid in the cell it is possible to determine the volume change of the specimen and the changes in the average cross-section that occur during testing.

The specimen is wrapped in a 5 mm thick rubber membrane which provides the waterproofing of the material, while an inner PVC foil prevents the membrane from being pierced by the rock grains.

As in the case of the oedometer, a back pressure system allows for the application of pore-pressures to the specimen as well as the measurements of the permeability of the test material.

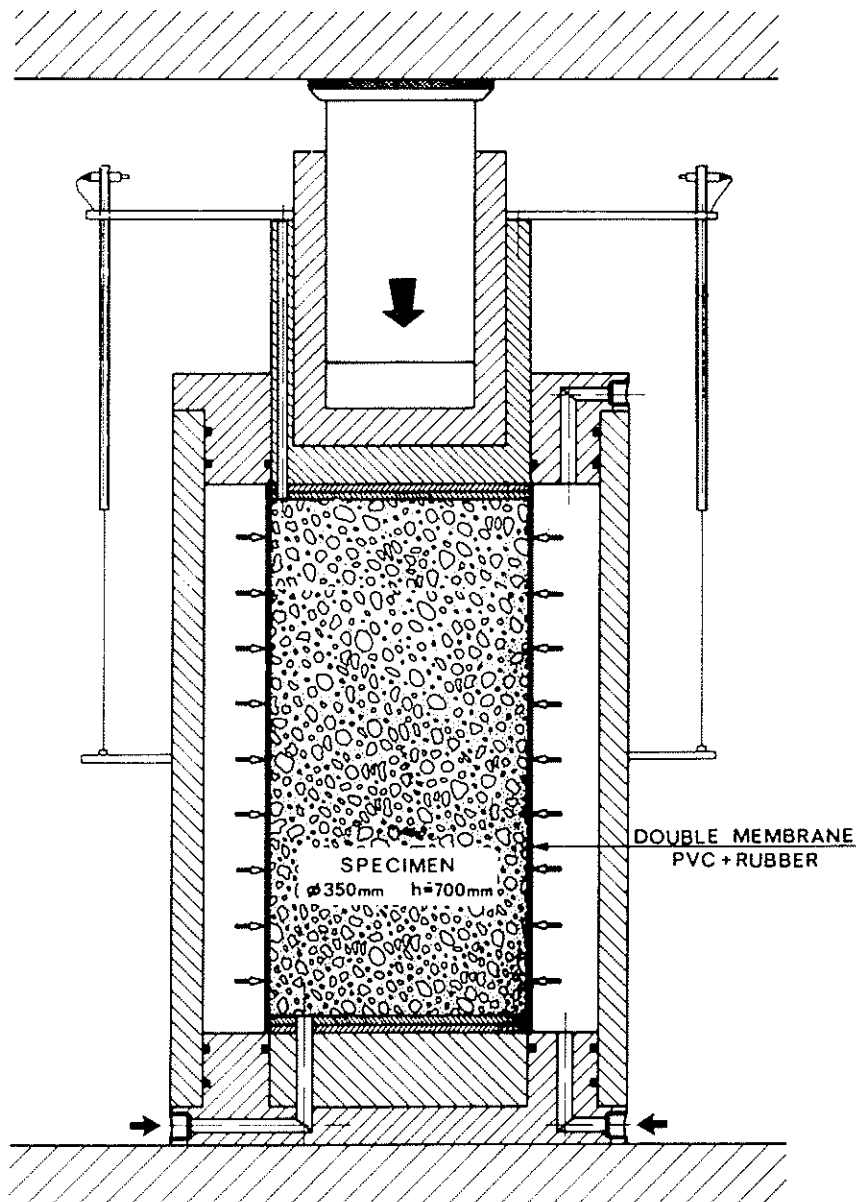


Fig. 3

Scheme of the triaxial cell ( $\varnothing = 350$  mm,  $H = 700$  mm).  
*Schéma de la cellule triaxiale ( $\varnothing = 350$  mm,  $H = 700$  mm).*

### 3. CRITERIA FOR SPECIMEN PREPARATION

As mentioned above, depending on the diameter of the chamber used, it may be necessary to scale down the grain size distribution curve of the examined material.

The scaling down can be realized by a simple translation of the curves following the criterion shown in Fig. 4.

The basic problem is to verify if the specimen obtained by this method is still representative of the mechanical behaviour of the real material. To give an exhaustive answer to this question ISMES carried out some years ago a vast research, testing the same type of material (granite) in cells with different diameters (100, 500, 1 300 mm). A constant value of 0.1 was adopted in this work for the ratio between maximum grain-size and cell diameter. Following this procedure, the specimens tested in the 3 different cells were obtained using grain size distribution curves reproduced with different scale ratios (Fig. 4).

For practical reasons the material with grain-size  $< 0,06$  mm was eliminated to prevent material from entering the drainage system of the chambers.

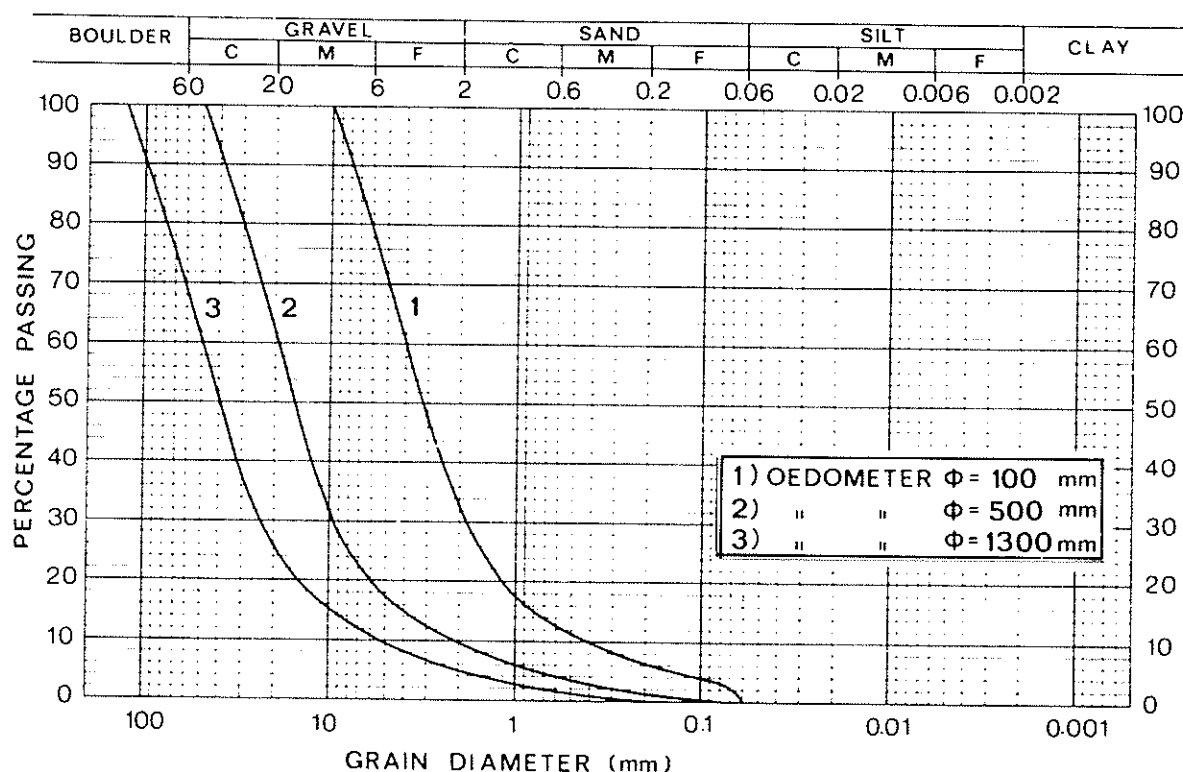


Fig. 4

Grading curves of granite utilized for tests in oedometers cells  
with different diameters

*Courbes granulométriques du granit utilisé pour les essais dans l'oédomètre  
avec différents diamètres*

The results of the comparative tests, carried out in the same conditions of void ratio,  $e$ , and shape coefficient,  $C_f$ , are summarized in Fig. 5 which shows the diagrams of axial load versus axial deformation.

The compression curves obtained with the different cells shows that the mechanical behaviour of the large specimens with diameter 500 and 1 300 mm is consistent while the compressibility of the smallest specimen is significantly lower.

The results of this comparative research seem to convalidate the correctness of the criteria adopted for the reduction of the gradings if test chambers with a diameter non less than 500 mm are used. It must also be observed that the compressibility of the material increases with increasing grain-size because of the effects of grain crushing during the test.

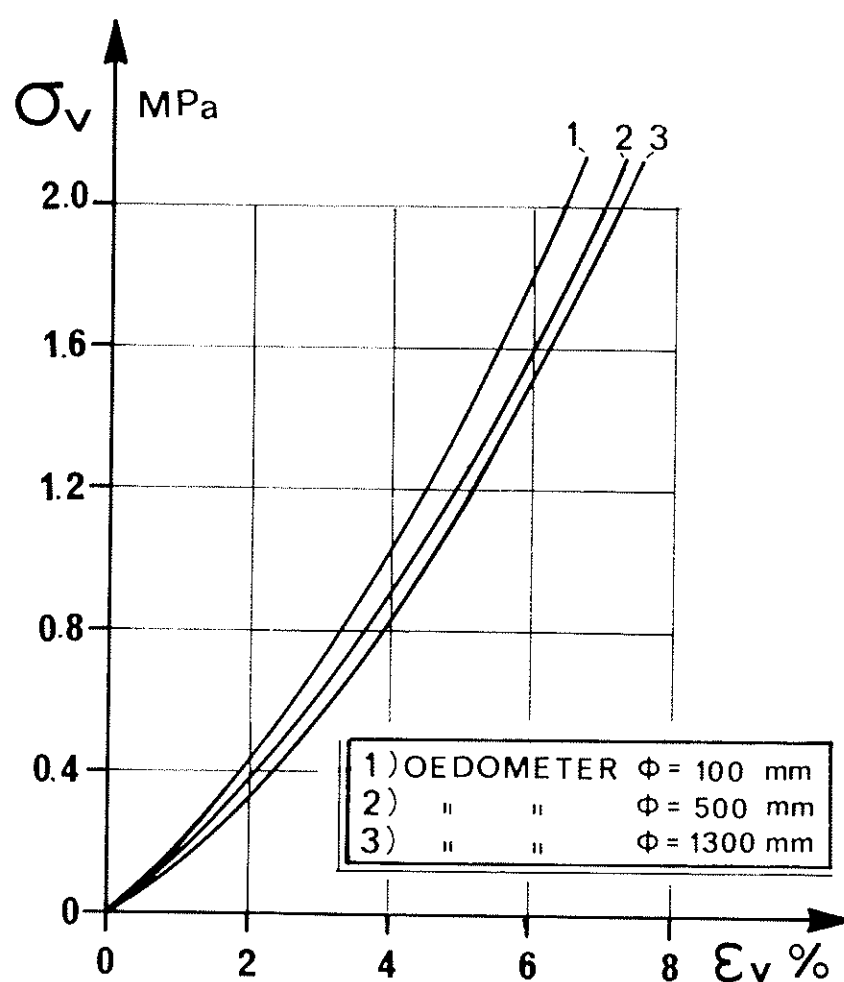


Fig. 5

Axial load versus axial deformation curves obtained with different oedometers in the same conditions of:

*Diagrammes charge axiale - déformation axiale obtenus avec différents œdomètres dans les mêmes conditions de :*

- |  |  |
|--|--|
| — ratio between maximum grain-size and cell diameter (0.1) | — rapport entre dimensions maximales des granulats de diamètre |
| — initial void ratio $e$ , = 29.0 %                        | — indice initial des vides $e$ , = 29,0 %                      |
| — shape coefficient $C_f$ , = 0.16.                        | — coefficient de forme $C_f$ , = 0,16                          |

Great care must be taken in the preparation of specimens for both oedometer and triaxial tests. The material with the desired grain-size curve is placed in layers and each layer is compacted by a special vibrating compactor provided with a small circular steel plate in order to obtain the desired initial density.

The preparation of the triaxial specimens is somewhat more complicated since it requires for the placing of the material a moulder which must be removed before the cell is mounted.

#### 4. INFLUENCE OF SOME PHYSICAL PARAMETERS ON THE COMPRESSIBILITY OF GRANULAR MATERIALS

One of the parameters which greatly influences the compressibility of a granular material is the initial void ratio. The importance of this parameters can be seen from Fig. 6 in which the results of 3 tests are shown

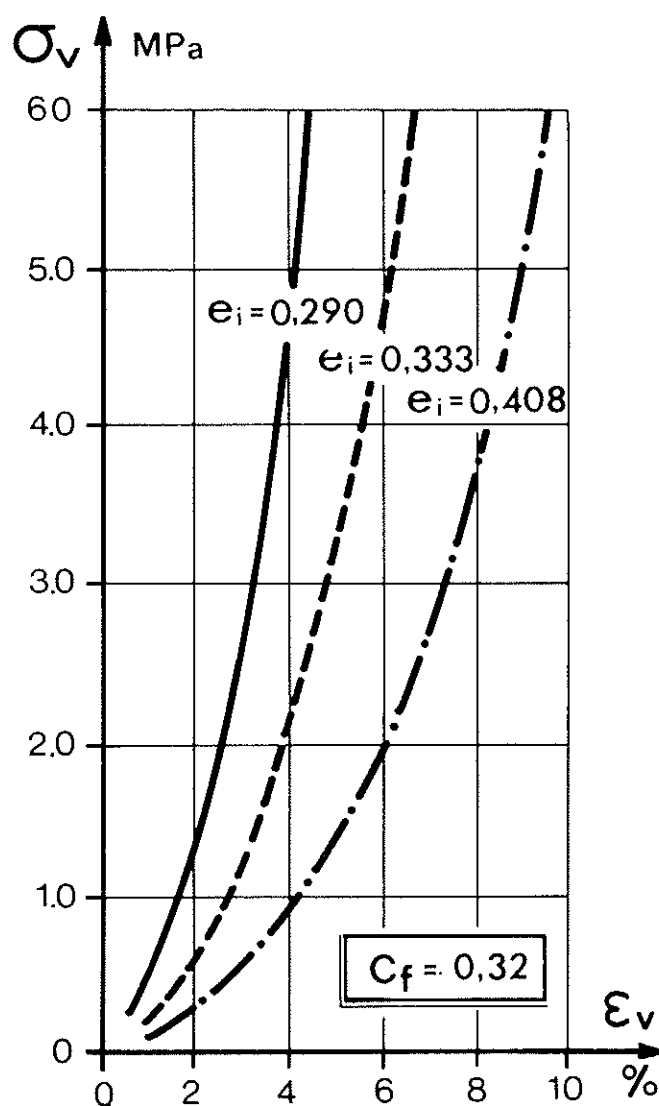


Fig. 6

Effect of initial void ratio ( $e_i$ ) on the compressibility of a rockfill of limestone.

*Effet de l'indice initial des vides ( $e_i$ ) sur la compressibilité d'un enrochement en calcaire.*



which were carried out on a rockfill of limestone in a  $\varnothing = 500$  mm cell. Three different values of the initial void ratio were examined.

Another parameter which influences the compressibility of the material is the shape coefficient,  $C_f$ , of the grains, defined as the ratio between the volume of a certain number of grains and the sum of the volumes of the corresponding circumscribing spheres. Fig. 7 shows the compressibility curves of limestone specimens which have different values of  $C_f$  but constant voids ratios.

It may be seen that the compressibility increases with increasing  $C_f$ , that is when the rock grains become rounder.

The presence of water plays also a fundamental role in the behaviour of granular materials. The compressibility is largely increased by saturation as can be seen in Fig. 8 which shows the results of two tests, 1 and 2, made on dry and saturated specimens of diorite. A third test (curve 3) was car-

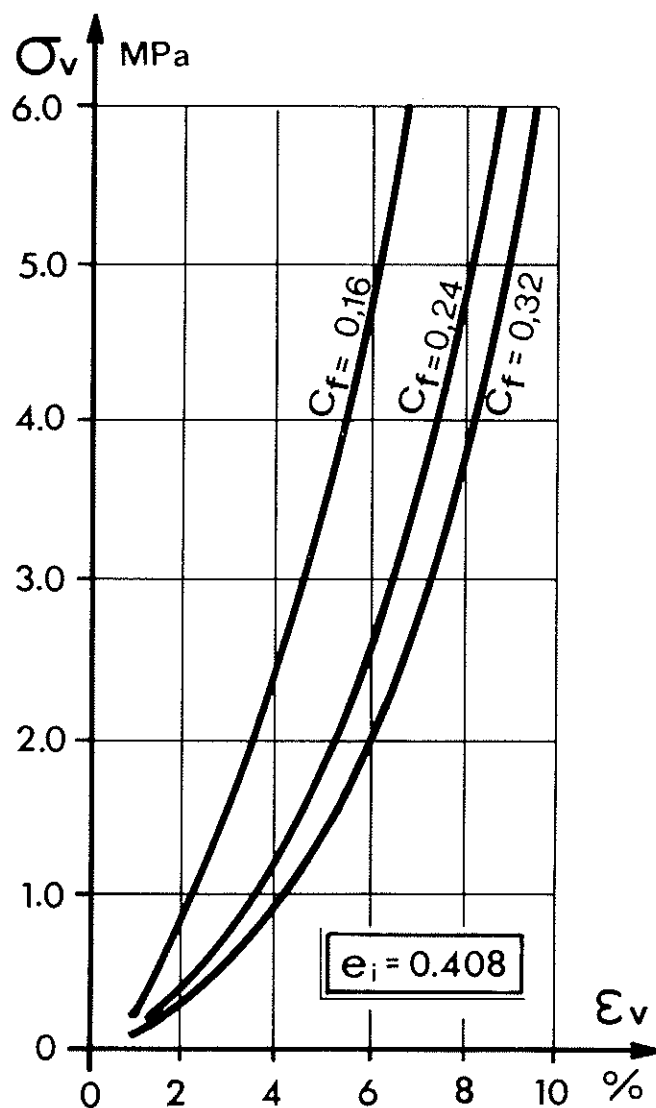


Fig. 7

Effect of shape coefficient ( $C_f$ ) on the compressibility of rockfill of limestone.  
*Effect du coefficient de forme ( $C_f$ ) sur la compressibilité d'un enrochement en calcaire.*

ried out on an initially dry specimens which was saturated under a constant load. It can be seen that after saturation the material follows curve 2 (of the initially saturated specimen) on further loading.

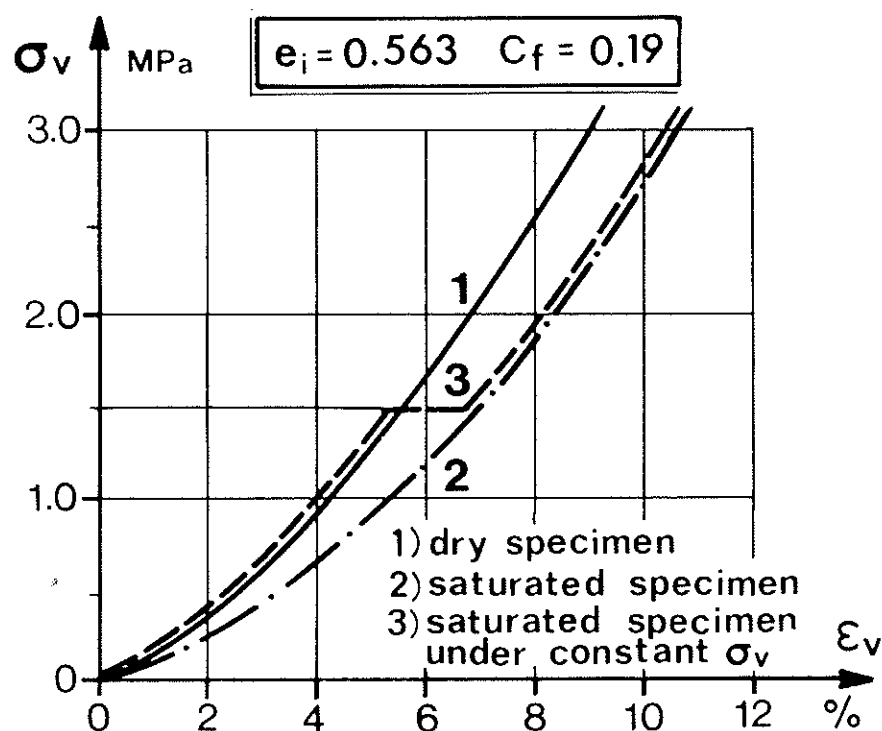


Fig. 8

Compression curves obtained on dry and saturated specimens of granite  
*Courbes de déformation obtenues sur échantillons secs et saturés de granit*

## 5. RESULTS OF TESTS ON SOME FILL MATERIALS

This chapter covers the results of a few oedometer and triaxial tests which have been carried out on the construction materials of four earth and rockfill embankments.

*Menta Dam* (Southern Italy) 80 m high rockfill dam with bituminous upstream deck.

*Las Cuevas Dam* (western Venezuela) 100 m high earthfill dam with central core.

*Deposit of Mine Tailings* (Italy) Tailings of fine sand, the residue of an ore-pulp resulting from the mechanical and chemical treatment of rock.

*Motorway Embankment* (Italy) Large rockfill embankment.

In all cases, the large scale laboratory tests were carried out in order to furnish representative design parameters for the stress-strain and, in one case, the permeability characteristics on the in situ materials.

## 5.1. MENTA DAM

### 5.1.1. Material

Rockfill from metamorphous formations of micashists and paragneiss with intrusions of pegmatite and quartz. This is a material which, when exploited in the quarry, breaks down easily along pre-existing planes of weakness to a coarse sandy gravel with cobbles. Grains are of elongated shape. Some basic characteristics of the material are listed below. Tested grain size distributions are shown in Fig. 9 together with a "field grading" determined by means of a full scale blasting test.

$C_f$ = (from a total of 50 examined grains) .....	0.228
$C_u$ = Coefficient of uniformity .....	9.8
$C_c$ = Coefficient of curvature .....	1.6
$G$ = Specific gravity of grains — dry .....	2.67
— bulk (saturated surface dry) ...	2.71
— bulk (apparent) .....	2.77
Water absorption (%) .....	1.37
Los Angeles abrasion resistance (%) .....	42.2
$B_r = a \cdot \sigma_v$ (Grain breakage factor) measured in oedometer:	$a = 0.833$

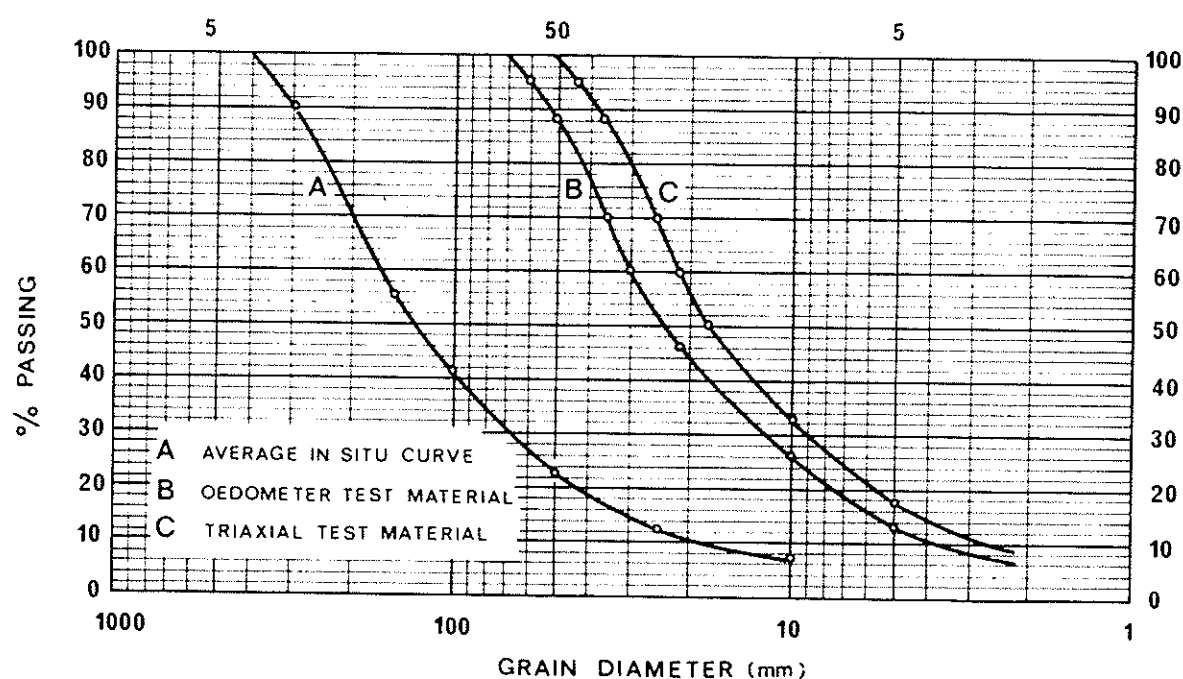


Fig. 9

Rockfill for Menta Dam: gradings

*Enrochement du barrage Menta: courbes granulométriques*

### 5.1.2. Large Scale Oedometer Tests

Four tests in a  $\varnothing = 500$  mm,  $h = 1000$  mm cell were carried out up to vertical pressures of 1.18 MPa (tests 1 and 2) and 2.33 MPa (tests 3 and 4) on samples which were first dry and then saturated during testing, or

samples which were saturated from the beginning (Fig. 10). Samples were prepared in five equal layers each of which was compacted by a small vibrating disk.

Unloading and reloading cycles were carried out. The compression curves are shown in Fig. 10, some of the measured parameters in Table 1. It will be noted that the material is rather compressible for a rockfill: tangent oedometer moduli vary between 10 and 40 MPa. On saturation the material undergoes large compressive strains of 8 — 12 % (8 % under vertical pressures of 1.2 MPa, 12 % under pressures of 2.33 MPa).

In this type of oedometer test the direct determination of the coefficient of earth pressure at rest,  $K_0$ , is possible because both  $\sigma_1$  and  $\sigma_3$  are measured during compression. An example of the variation of horizontal stress with vertical stress is shown in Fig. 11 for one of the tests carried out.

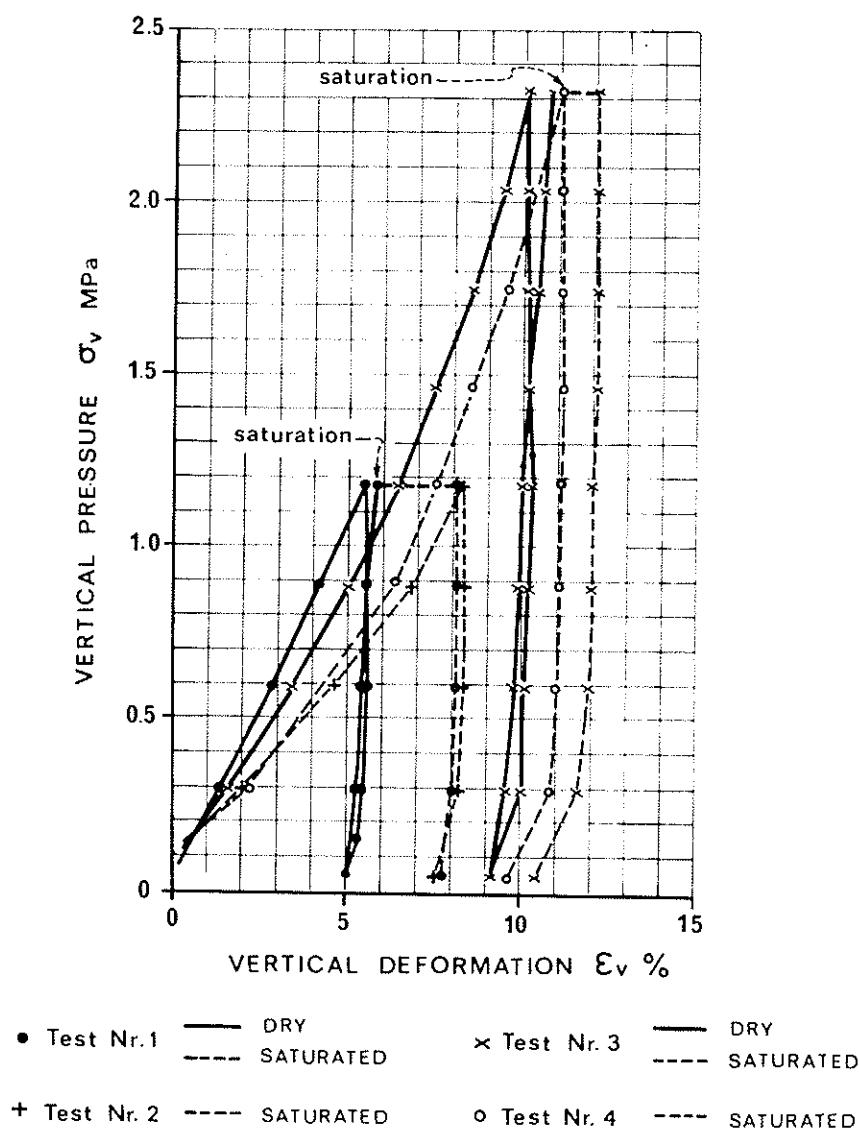


Fig. 10

Rockfill for Menta Dam - oedometer stress-strain curves

*Enrochement du barrage Menta - courbes contraintes-déformations des essais œdométriques*

TABLE 1

Rockfill of Menta dam - Parameters measured in oedometer tests

Test No.	$\gamma_{di}$ (g/cm <sup>3</sup> )	$\gamma_{df}$ (g/cm <sup>3</sup> )	$e_i$ —	$e_f$ —	$B_x$ (%)	$m$ —	$a$ —	RR —	$K_{onc}$ —	$\bar{\varphi}$ (°)	Material (*)
1	1.96	2.12	0.362	0.259	7.5	110	0.67	0.0076	0.361	39.7	<i>d</i>
2	1.97	2.13	0.355	0.255	7.5	36	0.21		0.336	41.6	<i>s</i>
3	1.96	2.19	0.362	0.221	16	110	0.67	0.011	0.340	41.3	<i>d</i>
4	1.96	2.17	0.362	0.231	15	36	0.21		0.350	40.5	<i>s</i>

(\*) *d* = sample dry, initially  
*s* = saturated, initially

where:

 $\gamma_{di,f}$  = initial/final dry density. $e_{i,f}$  = initial/final void ratio. $B_x$  = Grain breakage factor. $m$  = modulus number with regard to  $E_{vd}$ . $1 - a$  = modulus exponent with regard to  $E_{vd}$ .

RR = compression ratio.

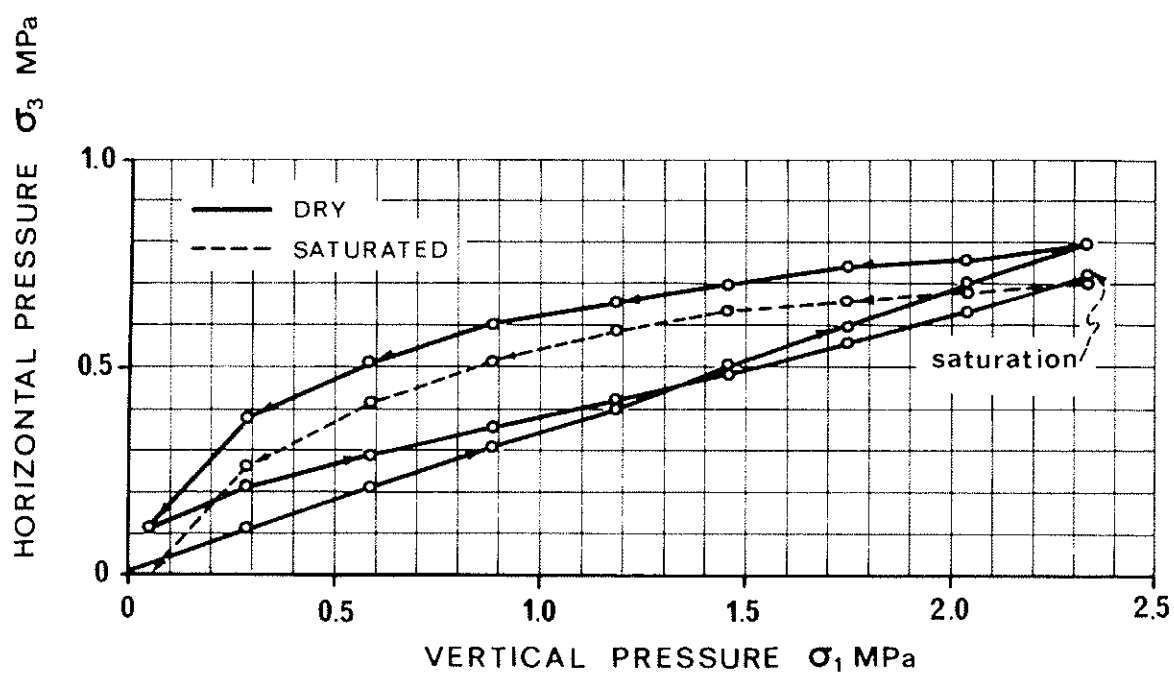
 $K_{onm}$  =  $K_0$  on first loading. $\varphi$  = angle of shearing resistance in terms of effective stress.

Fig. 11

Rockfill for Menta Dam - graph of  $\sigma_1$  versus  $\sigma_3$ Enrochement du barrage Menta - diagramme  $\sigma_1 - \sigma_3$

$K_0$  on first loading, called  $K_{0\ nc}$ , can be related to the friction angle,  $\bar{\varphi}$ , by the well-known relationship:

$$K_{0\ nc} = 1 - \sin \bar{\varphi}$$

It will be seen that the values of  $\bar{\varphi}$  which have thus been obtained and are listed in Table 1, are in good agreement with those measured in the triaxial compression tests (Table 2).

As far as the coefficient of earth pressure at rest on unloading,  $K_{0\ oc}$ , is concerned, it too can be correlated to  $K_{0\ nc}$ . One of the more widely used relationships is the following.

$$K_{0\ oc} = K_{0\ nc} \cdot OCR^b$$

where

$$\begin{aligned} OCR &= \text{overconsolidation ratio} \\ b &= \text{constant for a given soil} \end{aligned}$$

The exponent  $b$  has been found to be equal to 0.75 on average for the examined rockfill.

### 5.1.3. Large Scale Triaxial Tests

Two consolidated drained tests were carried out on  $\varnothing = 350$  mm,  $h = 700$  mm samples which were prepared in the same manner as for the oedometer tests. The confining pressure was in both cases 0.5 MPa. One sample was partly saturated (test No. 1), the other fully saturated (test No. 2). Shearing was carried a little beyond the peak resistance whence the samples were unloaded. Axial and volumetric strains were measured during the tests.

Measured parameters are shown in Table 2.

TABLE 2

Rockfill of Menta Dam - Parameters measured in triaxial tests

Test no.	$\gamma_{di}$ (g/cm <sup>3</sup> )	$e_i$ —	$\sigma_3$ MPa	$(\sigma_1 - \sigma_3)_{max}$ MPa	$\bar{\varphi}^*$ (°)	$\bar{c}^*$ MPa	$(\epsilon_a)_f$ (%)	$b_k$ (%)
1	2.0	0.335	0.5	2.1	42.6	0	8.4	17.5
2	2.0	0.335	0.5	1.84	40.4	0	9.0	20
(*) Failure envelope assumed to be linear and to pass through origin.								

$\sigma_3$  = minor principal stress.  
 $\sigma_1 - \sigma_3$  = deviatoric stress.

$\bar{c}$  = cohesion intercept.  
 $(\epsilon_a)_f$  = axial failure strain.

#### 5.1.4. Hyperbolic Stress-Strain Parameters

The description of the procedure for deriving hyperbolic stress-strain parameters is beyond the scope of this paper. The procedures used follow those outlined by Kondner (1963) Duncan-Chang (1970) and Wong-Duncan (1974). The pertinent constitutive laws are listed in the Appendix.

The evaluated hyperbolic stress-strain parameters are listed in Table 3.

It can be seen that the results from the oedometer and triaxial tests are in good agreement. In addition to the already mentioned consistency in the measured values, moduli numbers,  $m$  and  $K$ , are in both types of test much larger for the dry material, while the moduli exponents,  $1-a$  and  $n$ , are larger in the case of the saturated material.

TABLE 3

Rockfill of Menta Dam — Hyperbolic stress-strain parameters

Parameter	Unit	Material dry	Material Saturated
$K$	—	265	135
$K_{ur}$	—	1700	900
$n = n_{ur}$	—	0.50	0.71
$\phi$	(°)	42.6	40.4
$\bar{c}$	MPa	0	0
$R_f$	—	0.6	0.54
$G$	—	0.25	0.25
$F$	—	0.09	0.09
$d$	—	8.2	8

- $K$  = modulus number with regard to  $E_v$ .  
 $K_{ur}$  = modulus number for unloading-reloading.  
 $n$  = modulus exponent with regard to  $E_v$ .  
 $n_{ur}$  = modulus exponent for unloading-reloading.  
 $R_f$  = failure ratio.  
 $G, F, d$  = Poisson's ratio parameters.

## 5.2. LAS CUEVAS DAM

### 5.2.1. Materials

- (A) Sandstone from the sedimentary Rio Negro formation, a very weakly cemented friable rock which breaks down to a uniform medium to fine sand when exploited and used as construction material for an earth dam. Sand grains consist mainly of quartz, the cementing agent of kaolinite.
- (B) Closely interbedded layers of the above sandstone, with a more or less pronounced silt content, and shale (lutite) composed mainly of quartz, kaolinite and mica. When handled as construction material this rock becomes a heterogeneous mix of lumps of shale and silty sand.

Classification test results for the sand and the shale are listed below. Representative grain size-distributions for material A and B are shown in Fig. 12.

Sandstone :

$$C_u = 5.5$$

$$G = 2.66$$

Shale :

$$G = 2.60$$

$$LL = 38 \text{ (liquid limit)}$$

$$LP = 21 \text{ (plastic limit)}$$

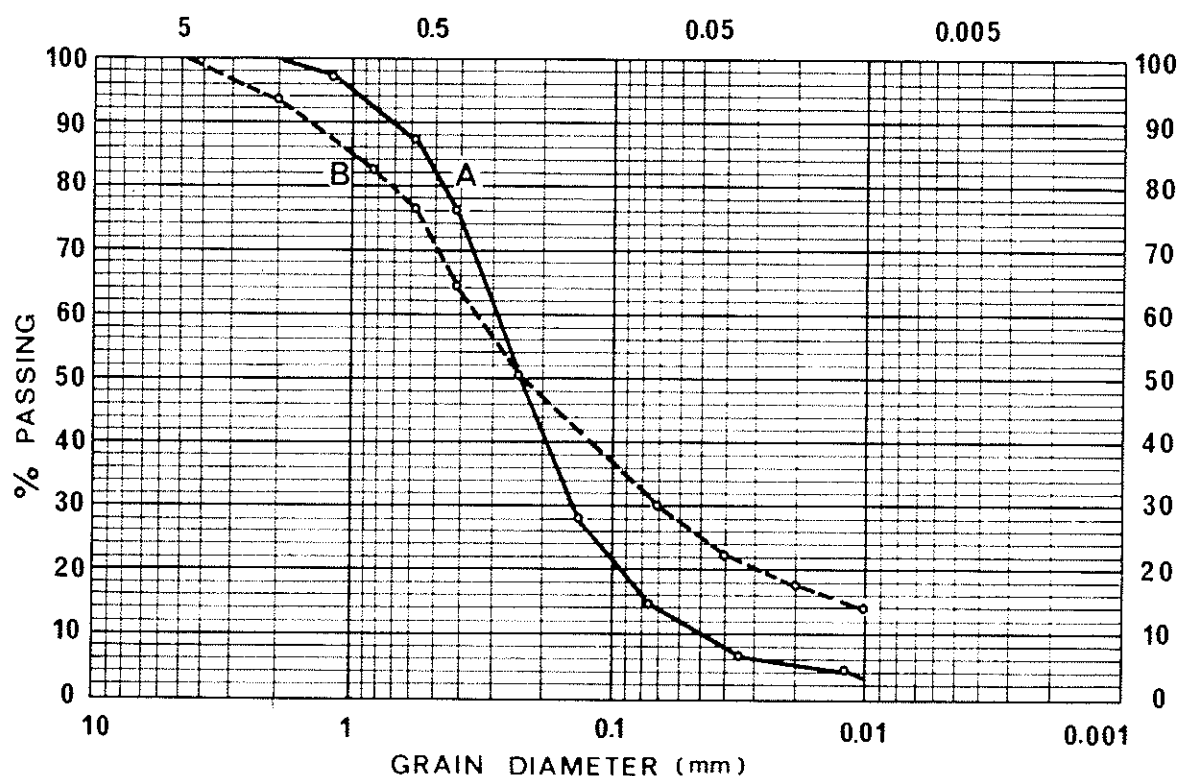


Fig. 12

Las Cuevas Dam - materials grading  
Barrage Las Cuevas - granulométries des matériaux

### 5.2.2. Large Scale Oedometer Tests

One oedometer test in a  $\varnothing = 600$  mm,  $h = 1\,200$  mm cell, with unloading and reloading cycles, was carried out on each of the above described materials, A and B. Maximum loads were 2.82 and 2.46 MPa, respectively. Samples were prepared at a prefixed moisture content in 18 equal layers and compacted with a small vibrating disk. At some stage during the test they were saturated by back pressure. Constant head permeability tests were carried out under various vertical loads. Flow of water was vertically upward in these test, the hydraulic gradients equal to 9 and 18 in the case of material A and round 29 in the case of material B.



The compression curve for material A is shown in Fig. 13. The variation of the oedometer modulus,  $E_{ed}$ , with vertical pressure is shown in the same figure. Some of the measured parameters are listed in Table 4, permeability coefficients in Table 5.

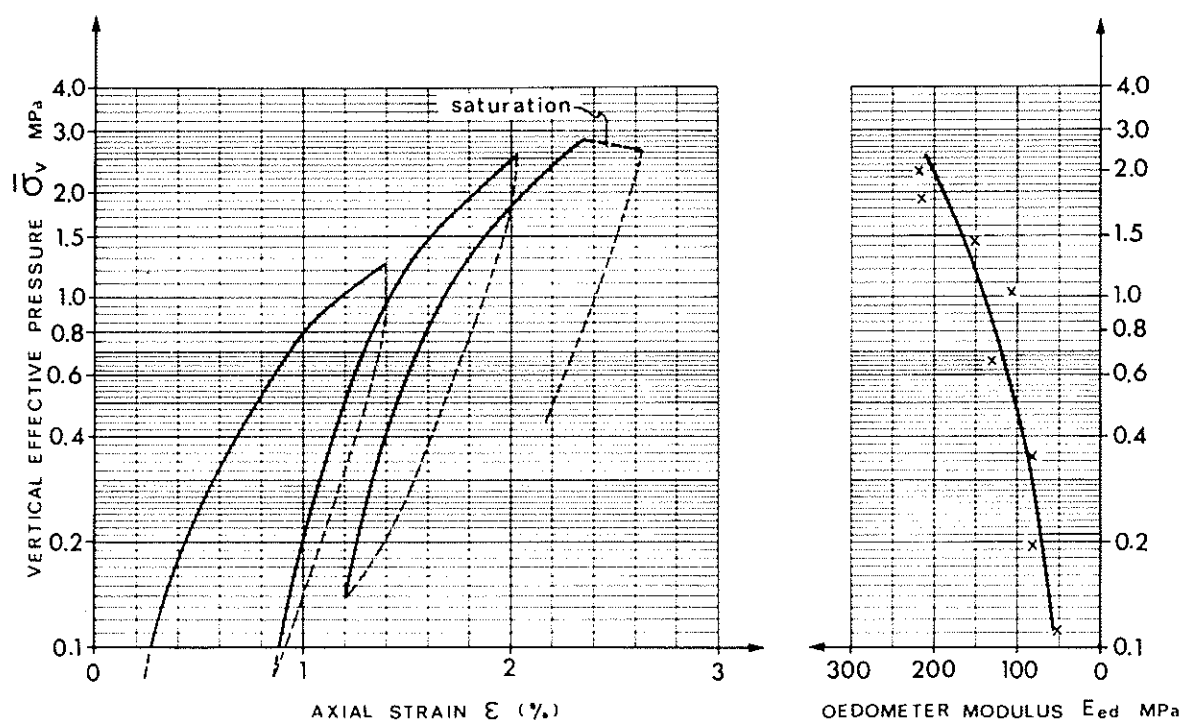


Fig. 13

Las Cuevas Dam: material A - oedometer stress-strain curve  
and plot of oedometer modulus versus vertical pressure

Barrage Las Cuevas : matériau A - courbe contrainte-déformation  
et diagramme module œdométrique-pression verticale

TABLE 4

Las Cuevas Dam materials — Parameters measured in oedometer tests

Material	$\gamma_{ds}$ (g/cm <sup>3</sup> )	$w_i$ (%)	$e_i$ —	$m$ —	$a$ —	CR —	RR —	$K_{mc}$
A (moist)	1.82	12.2	0.463	530	0.574	0.021	0.006	0.34
B (saturated immed. after beginning)	1.72	14.2	0.564	42	0.183	0.100	0.008	0.52
$w_i$ = Initial moisture content. CR = Compression ratio.								

TABLE 5

Las Cuevas Dam materials - Permeability measured in the oedometer

Material	Load Condition	Vertical Effective Pressure MPa	Hydraulic Gradient (—)	Dry density $\gamma_d$ (g/cm <sup>3</sup> )	Coeff. of permeability $k$ (cm/s . 10 <sup>-5</sup> )
A	Unloading	2.21	9.1	1 867	13.1
	—	1.37	18.1	1 865	12.9
	—	0.85	9.0	1 860	13.0
	—	0.85	18.0	1 859	12.1
B	Loading	0.79	28.3	1.84	5.3
	—	1.23	28.6	1 857	3.6
	—	1.65	29.0	1 882	2.0
	—	2.05	29.3	1 905	1.4
	—	2.46	29.6	1 919	1.0
	Unloading	2.04	29.6	1 918	1.1
	—	1.63	29.5	1 917	1.1
	—	1.20	29.5	1 916	1.2
	—	0.76	29.4	1 911	1.2

### 5.2.3. Hyperbolic Stress-Strain Parameters

No triaxial compression test results are available so far for the materials under consideration. Nevertheless, the determination of the modulus number,  $K$ , and exponent,  $n$ , is still possible as Clough and Duncan (1969) have shown if the parameters  $\bar{c}$ ,  $\bar{\varphi}$  and  $R_f$  are assumed to be known. The relevant relationships are listed in the Appendix. In the present case the cohesion intercept,  $\bar{c}$ , can safely be assumed to be zero for both materials and the angle of shearing resistance,  $\bar{\varphi}$ , can with sufficient accuracy been estimated through the coefficient of earth pressure at rest which is known from the measurements of  $\sigma_1$  and  $\sigma_3$ :

$$K_0 = 1 - \sin \bar{\varphi}$$

$R_f$  is unknown, but a reasonable range of values can be estimated from the available literature (Wong and Duncan, 1974).

Table 6 shows the values of  $K$ ,  $K_{ur}$ ,  $n$  and  $n_{ur}$  which have been evaluated. It will be seen that in the case of material A the correct value of  $R_f$  is more likely to be close to the lower limit of the considered range, that is close to 0.65, since otherwise excessively high  $K$  values will result, while higher  $R_f$  values appear to be more appropriate for material B.

### 5.3. MINE TAILINGS

This case is reported here since it is another example which shows good agreement between values derived from oedometer tests and values measured in conventional shear tests, in this case shear box tests.

TABLE 6

Las cuevas Dam materials — Stress-strain parameters

Material	$K_0$ (—)	$\bar{\varphi}$ (°)	$\bar{c}$ MPa	$n = n_{ur}$ (—)	K			$K_{ur}$ (—)
					$R_f = 0.65$	$R_f = 0.75$	$R_f = 0.85$	
A	0.34	41	0	0.517	1407	1641	1938	2020
B	0.52	29	0	0.817	84	121	144	1080

### 5.3.1. Material

Uniform fine to medium sand which is the residue of the milling and chemical treatment of a quartzose tuff. The material has the following characteristics:

% passing ASTM sieve No. 200 .....	9 %
$C_u$ .....	3.25
$G$ .....	2.725
$\gamma_{d \max}$ .....	1.72 g/cm <sup>3</sup>
$\gamma_{d \min}$ .....	1.34 g/cm <sup>3</sup>

### 5.3.2. Large Scale Oedometer Test

A single test was carried out on a sample which was prepared moist at a water content of 8 % and compacted by vibrating disk in 4 layers to a dry density of 1.65 g/cm<sup>3</sup> and a void ratio of 0.65. The coefficient of earth pressure at rest,  $K_0$ , was measured as 0.37. Introducing this value into the equation

$$K_0 = 1 - \sin \bar{\varphi}$$

a value of  $\bar{\varphi} = 39^\circ$  is obtained for the friction angle. The shear box tests, on the other hand, resulted in the following friction angles:

$$\begin{aligned} \gamma_d = 1.32 & \quad \bar{\varphi} = 38^\circ \text{ (3 tests)} \\ \gamma_d = 1.45 & \quad \bar{\varphi} = 38^\circ \text{ (3 tests)} \end{aligned}$$

## 5.4. MOTORWAYS EMBANKMENT

### 5.4.1. Material

Rockfill consisting of sound angular pieces of gneiss. Test gradings were scaled down according to the criteria given in paragraph 3; the ratio between maximum grain size and sample diameter was chosen equal to 0.10.  $C_f$  was measured as 0.187, the dry specific gravity of the rock grains as 2.653.

### 5.4.2. Large Scale Oedometer Tests

Two tests were carried out on dry material in two cells of different size, viz.  $\varnothing = 100$  mm,  $h = 200$  mm and  $\varnothing = 500$  mm,  $h = 1\ 000$  mm. Both samples had the same initial void ratio,  $e_i = 0.553$ , and dry density,  $\gamma_{di} = 1.708$  g/cm<sup>3</sup>.

Vertical loads were carried up to 3.3 and 3.0 MPa, respectively. No unloading-reloading cycles were made.

The measured deformation parameters are shown in Table 7.

TABLE 7

Rockfill of gneiss — Deformation parameters

Parameter	Unit	Oedometer		Triaxial CD	
		$\varnothing = 100$ mm	$\varnothing = 500$ mm	$\varnothing = 100$ mm	$\varnothing = 350$ mm
$m$	—	217	160	—	—
$a$	—	0.75	0.68	—	—
K	—	518	438	338	256
$n$	—	0.25	0.32	0.40	0.47
$\varphi$	(°)	—	—	45-40(*)	43-39(*)
$c$	MPa	—	—	0	0
$R_f$	—	—	—	0.64	0.68
G	—	—	—	0.20	0.26
F	—	—	—	0.05	0.10
$d$	—	—	—	4.8	5.5
(*) Failure envelope curve.					

### 5.4.3. Large Scale Triaxial Tests

Again, tests were performed in two cells of different size with dimensions  $\varnothing = 100$  mm,  $h = 200$  mm and  $\varnothing = 350$  mm,  $h = 700$  mm. The tests were of the consolidated drained type and were carried out on dry material. The initial void ratios and dry densities that were achieved on sample preparation were exactly the same as in the case of the oedometer samples. The confining pressure,  $\sigma_3$ , ranged from 0.3 to 2.0 MPa. The tests were carried well beyond peak resistance. Beside axial and volumetric strains, also mean sample diameters were recorded (Fig. 14). Note that the graphs shown in the figure include the consolidation stage of the samples (under an isotropic pressure equal to the given value of  $\sigma_3$ ).

It will be seen that the initial volume decreases to a minimum, which is reached at the same strain as the peak strength, then becomes constant. As regards the mean cross-section, it may be observed that there is an initial decrease, then a rapid increase. It is interesting to note that the peak

strength occurs when the mean cross-section practically reverts to its initial value.

The derived stress-strain and shearing resistance parameters are shown in Table 7.

It will be noted that the moduli numbers (for conditions of both one-dimensional and triaxial compression) are consistently large for the small samples — by some 20-30 % — while the exponents are slightly larger for the bigger samples. The angles of shearing resistance,  $\bar{\varphi}$ , are also slightly smaller for the larger samples.

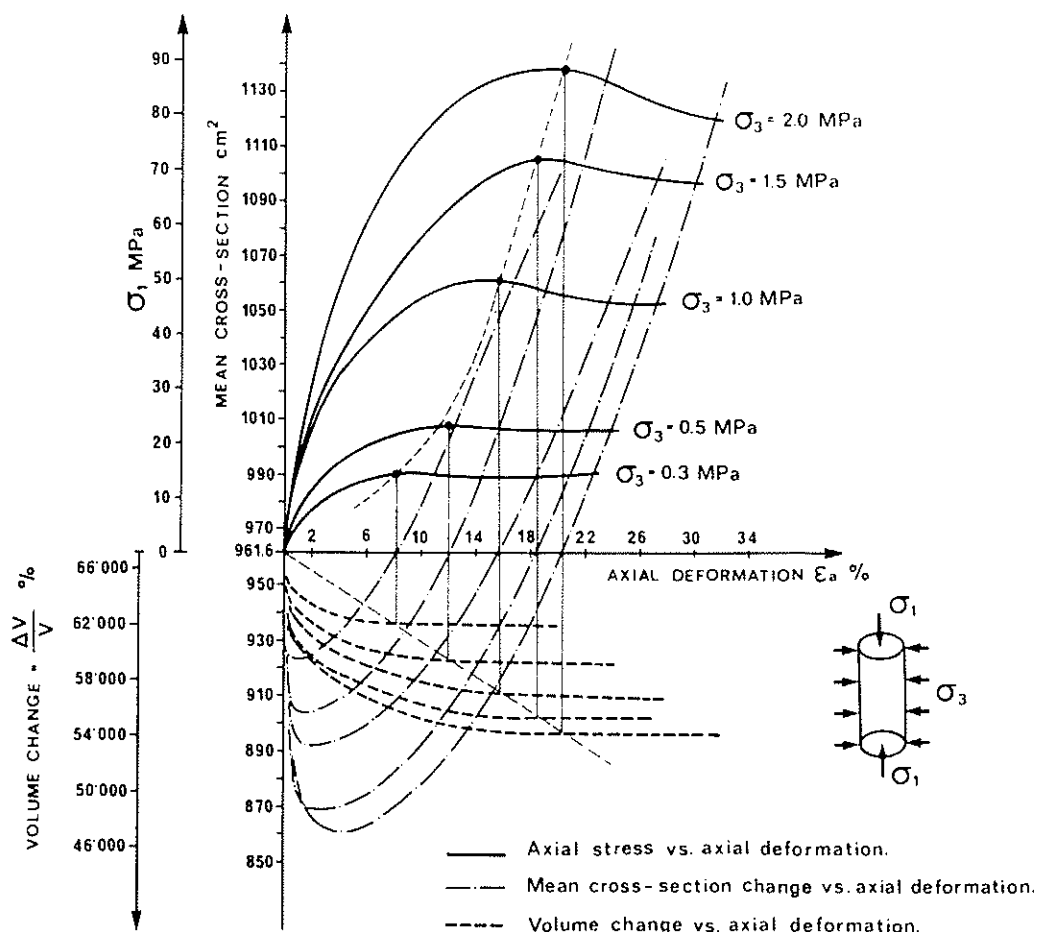


Fig. 14

Rockfill of gneiss - typical triaxial test results  
*Enrochement en gneiss - résultats types d'essais triaxiaux*

## A. APPENDIX — STRESS-STRAIN RELATIONSHIPS

## A.1. TRIAXIAL COMPRESSION TESTS

*Stress-Strain Curves*, Kondner, (1963) noted that stress-strain curves can be approximated by a hyperbola:

$$(\sigma_1 - \sigma_3) = \frac{\epsilon}{\frac{1}{E_i} + \frac{\epsilon}{(\sigma_1 - \sigma_3)_{ult}}}$$

The initial tangent modulus,  $E_i$ , is a function of the confining pressure  $\sigma_3$ , as shown by Janbu (1963):

$$E_i = K p_a \left( \frac{\sigma_3}{p_a} \right)^n \quad p_a = \text{reference pressure (1 atm)}$$

According to Mohr Coulomb's failure criterion:

$$(\sigma_1 - \sigma_3)_f = \frac{2 \bar{c} \cos \bar{\varphi} + 2 \sigma_3 \sin \bar{\varphi}}{1 - \sin \bar{\varphi}}$$

$(\sigma_1 - \sigma_3)_{ult}$  is reached at infinit strain only; thus it is always larger than the deviator stress at failure  $(\sigma_1 - \sigma_3)_f$ . The ratio  $R_f = \frac{(\sigma_1 - \sigma_3)_f}{(\sigma_1 - \sigma_3)_{ult}}$  is called failure ratio.

The tangent modulus at a given stress level,  $\sigma_1 - \sigma_3$ , is obtained by differentiating the first equation above:

$$E_t = \left[ 1 - \frac{R_f (\sigma_1 - \sigma_3)}{(\sigma_1 - \sigma_3)_f} \right]^2 E_i$$

Hence:

$$E_t = \left[ 1 - \frac{R_f (1 - \sin \bar{\varphi}) (\sigma_1 - \sigma_3)}{2 \bar{c} \cos \bar{\varphi} + 2 \sigma_3 \sin \bar{\varphi}} \right]^2 K p_a \left( \frac{\sigma_3}{p_a} \right)^n$$

*Unloading-reloading Modulus.* — In the same manner as the initial tangent modulus, the unloading-reloading modulus,  $E_{ur}$ , can be expressed as follows:

$$E_{ur} = K_{ur} p_a \left( \frac{\sigma_3}{p_a} \right)^{n_{ur}}$$

*Poisson's Coefficient.* — Volume changes measured during triaxial tests can be used for the evaluation of Poisson's ratio:

$$\epsilon_a = \frac{-\epsilon_r}{\nu_i - d \cdot \epsilon_r} \quad \begin{array}{l} \epsilon_a = \text{axial strain} \\ \epsilon_r = \text{radial strain} \end{array}$$

The variation of the initial Poisson's ratio (at zero strain),  $\nu_i$ , varies with the confining pressure,  $\sigma_3$ , as follows:

$$\nu_i = G - F \log_{10} \frac{\sigma_3}{p_a}$$

The instantaneous slope of the curve representing the variation of  $\epsilon_a$  with  $\epsilon_{is} = \nu_i$ . This last parameter called tangent value of Poisson's ratio, may be expressed in terms of stresses as follows:

$$\nu_i = \frac{G - F \log \frac{\sigma_3}{p_a}}{\left[ 1 - \frac{d \cdot (\sigma_1 - \sigma_3)}{K p_a \left( \frac{\sigma_3}{p_a} \right)^n \left[ 1 - \frac{R_i (\sigma_1 - \sigma_3) (1 - \sin \bar{\varphi})}{2 \bar{c} \cos \bar{\varphi} + 2 \sigma_3 \sin \bar{\varphi}} \right]} \right]^2}$$

## A.2 OEDOMETER TESTS

### *Oedometer Modulus*

$$E_{ed} = \frac{\Delta p}{\Delta \epsilon}$$

In analogy to the correlation N between  $E_i$  and  $\sigma_3$  used in the case of the triaxial tests,  $E_{ed}$  can be related to the vertical pressure (Janbu, 1963):

$$E_{ed} = m \cdot p_a \left( \frac{p}{p_a} \right)^{1-a}$$

*Tangent Modulus* (Chang + Duncan, 1970)

$$E_t = E_{ed} \left[ 1 - \frac{2 K_o^2}{1 + K_o} \right]$$

The stress level during primary loading in a consolidation test is determined as follows:

$$\bar{\sigma}_3 = K_o p = K_o \cdot \bar{\sigma}_1$$

and

$$\sigma_1 - \sigma_3 = \bar{\sigma}_3 \left( \frac{1 - K_o}{K_o} \right)$$

Substituting into the relationships of paragraph A.1 (Triaxial Compression Tests), one obtains correlations for the determination of stress-strain parameters from oedometer tests. The resulting equation for the initial tangent modulus,  $E_i$ , has been given by Clough and Duncan (1969):

$$E_i = \frac{\frac{\Delta p (1 + e_o)}{\Delta e} \left[ 1 - \frac{2 K_o^2}{1 + K_o} \right]}{\left[ 1 - \frac{p (1 - K_o) R_i}{K_o p \left[ \tan^2 \left( 45^\circ + \frac{\bar{\varphi}}{2} \right) - 1 \right] + 2 \bar{c} \tan \left( 45^\circ + \frac{\bar{\varphi}}{2} \right)} \right]^2}$$

## REFERENCES

- [1] BERTACCHI, BELLOTTI. — Experimental research on materials for rock-fill dams. *Proced. 10 ICOLD Congress Montreal, Canada*, (1970).
- [2] CHANG, DUNCAN. — Analysis of Soil Movement around a Deep Excavation *Proc., ASCE Vol. 96, NO.SM5* (1970).
- [3] CLOUGH, DUNCAN. — Finite Element Analyses of Port Allen and Old River Locks; U.S. Army Engineers Waterways Experiment Station, Corps of Engineers, Vicksburg, Mississippi (1969).
- [4] DUNCAN, CHANG. — Nonlinear Analysis of Stress and Strain in Soils *Proc. ASCE, Vol. 89, NO.SM1* (1970).
- [5] FUMAGALLI. — Tests on Cohesionless Material for Rockfill Dams *Proc. ASCE, January* (1969).
- [6] FUMAGALLI, MOSCONI, ROSSI. — Laboratory Tests on Materials and Static Models for Rockfill Dams *Proc. 10 ICOLD Congress Montreal, Canada* (1970).
- [7] JANBU. — Soil Compressibility as Determined by Oedometer and Triaxial Tests, *European Conf. on Soil Mech. and Found. Eng., Wiesbaden, Vol. 1* (1963).
- [8] KONDNER. — Hyperbolic Stress-Strain Response of Cohesive Soils, *Proc. ASCE, Vol. 89, No. SM1* (1963).
- [9] ROSSI. — The Study of Rockfill Dams Problems: Physical Models and Tests on Granular Materials *Proc. Colloq. on Geomech. Models ISMES, March* (1979).

## SUMMARY

This paper presents some testing apparatuses designed and constructed by ISMES for determining the mechanical properties of granular materials for embankment dams.

Special attention is devoted to a special oedometer cell (diam. up to 130 cm), with deformable lateral wall in axial direction. The cell makes it possible to avoid the friction effect that generally affects the tests carried out by oedometer cell with rigid walls.

Up-to-date apparatuses make it possible both to apply a back-pressure to the material and to determine permeability characteristics under different stress conditions.

Oedometer cell test results are compared with those obtained by conventional triaxial tests carried out on specimens  $\varnothing = 35$  cm,  $H = 70$  cm.

To illustrate the criteria adopted for reproducing, on reduced-scale, the grading curve of materials, the most significant results, obtained from



an extensive series of calibration tests performed on various-diameter cells, are shown.

Lastly, the paper presents the results of tests carried out within the design of some embankments for two rockfill dams, a deposit of mine tailings and a motorway.

The processing of the results, in order to determine stress-strain characteristics of materials in question, is also presented in detail.

## RÉSUMÉ

Ce rapport présente quelques dispositifs d'essai projetés et réalisés par ISMES pour la détermination des caractéristiques mécaniques des matériaux granulaires pour la construction de barrages en remblai.

On a accordé une attention particulière à un œdomètre spécial (jusqu'à 130 cm de diamètre), avec paroi latérale axialement déformable qui permet d'éliminer les phénomènes de frottement qui interviennent normalement dans les essais effectués avec œdomètre à paroi rigide.

Des dispositifs récents permettent : soit d'effectuer des essais de compressibilité avec pression interstitielle, soit de déterminer les caractéristiques de perméabilité sous différentes conditions de contrainte.

Les résultats des essais avec œdomètre sont comparés avec ceux obtenus avec essais triaxiaux conventionnels effectués sur échantillons de diamètre  $\varnothing = 35$  cm et hauteur  $H = 70$  cm.

Pour illustrer les critères adoptés pour la reproduction à l'échelle réduite de la courbe granulométrique du matériau, on reporte les résultats plus significatifs obtenus à travers une vaste série d'essais de calibration effectués sur œdomètres avec différents diamètres.

Enfin, on donne les résultats d'essais effectués pour l'établissement des projets de remblais pour deux digues, un barrage de stériles miniers et une autoroute.

L'élaboration des résultats afin de déterminer les caractéristiques contraintes-déformations des matériaux en question est également présentée en détail.

